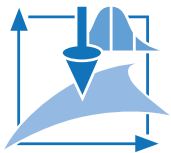


Objective Specifications of Terrestrial Laserscanners – A Contribution of the Geodetic Laboratory at the Technische Universität München

Prof. Dr.-Ing. Thomas Wunderlich, Dr.-Ing. Peter Wasmeier,
Johannes Ohlmann-Lauber, Thomas Schäfer, Fabian Reidl

Blue Series Books at the Chair of Geodesy, Volume 21, 03/2013

Objective Specifications of Terrestrial Laserscanners –
A Contribution of the Geodetic Laboratory at the Technische Universität München



Univ.-Prof. Dr.-Ing. habil. Thomas A. Wunderlich

Technische Universität München
Faculty of Civil Engineering and Surveying
Institute of Geodesy, GIS and Land Management
Chair of Geodesy

Arcisstraße 21
80290 Munich
Germany

Tel.: +49.89.289.22850

Fax: +49.89.289.23967

Mail: geodaesie@bv.tum.de

URL: <http://www.geo.bv.tum.de>

2013

ISBN 978-3-943683-21-9



Abstract

In geodesy, mandatory regulations on standardized specifications of terrestrial laserscanners' performance features are still missing which would allow an objective comparability of different scanner models. In this paper feasibly realizable testing series are presented, which will support such comparability using objective criteria. Basic concept especially is a relevant question for users concerning the quality of a TLS-generated 3D point cloud at plane surfaces and edges as a function of the chosen scanning filter setup. The comparison concept is applied using three up-to-date TLS systems (Faro Focus^{3D}, Leica HDS7000 and Leica Scanstation P20) and results are presented. One particular intent is to show a set of test arrangements for practical use to obtain system independent benchmarks describing quality features rather than using the pure manufacturers' technical data specifications. Furthermore at the beginning an overview on an existing TLS standard testing procedure is given.



Table of Contents

Abstract.....	3
Table of Contents.....	4
1 Preface	5
2 Existing concept of a TLS testing procedure	6
2.1 Probing error	6
2.2 Sphere-radius error	7
2.3 Sphere-spacing error	7
2.4 Resolution power	7
3 Practical TLS comparison series	8
3.1 Scan quality settings.....	8
3.2 TLS comparison conceptual design	8
3.3 Comparison parameter accuracy	8
3.4 Comparison parameter geometric truth	12
3.5 Effective working range	15
3.6 Measurement speed	17
4 TLS systems compared (scanners and software)	18
4.1 Data conversion and import filter settings.....	18
4.2 Tested scan quality settings	19
4.3 TLS testing track Eichenau	20
4.4 TLS testing field Munich	21
4.5 Precision (noise).....	22
4.6 3D accuracy	28
4.7 Calibration parameters.....	28
4.8 Edge behavior	29
4.9 Working range.....	32
4.10 Time of data acquisition.....	33
4.11 Impact of potential obstructions at the specimens	33
4.12 Summary	34
5 Outlook	35
Literature	36



1 Preface

The terrestrial laserscanner (TLS) market is fast-paced which leads to a great variety of measurement systems and a nearly annual reissue of well-known models showing more and more promising specifications. Generally speaking, all systems can be found working reliably and suitably for the all-day geodetic needs. But when investing in a new instrument, especially this “all-day work” needs to get a closer look to find the individual optimal buying decision. The major numbers usually obeyed here seem to be measurement speed and range which are placed very effectively in advertising by the manufacturers. But usually measurement speed is connected to smoothing filter influences as filtering is applied directly to the raw data during the measurement process. As a rule, the user has no access to the unfiltered data then, so inevitably the question on geometry truth and detail reproduction losses (e.g. when scanning edges) arises when these filters become effective. Thus, how significant are the manufacturers’ specification numbers when being compared – especially for anyone’s individual surveying task and accuracy expectations?

Mandatory regulations on standardized specifications of terrestrial laserscanners’ performance features are still missing which would allow an objective comparability of different scanner models (e.g. STAIGER 2005 and WUNDERLICH 2012). Besides the standardization of specifications in terms of a laboratory TLS testing procedure (KERN 2010, GOTTWALD ET AL. 2008), based on work of HEISTER (2006) the geodetic user community for many years is exerting for standardized field testing procedures to ensure usability right before usage (GOTTWALD ET AL. 2008, GOTTWALD 2008, TÜXSEN 2008 und WEHMANN 2008). Also to be mentioned is a currently being developed DVW (German surveyors’ association) consultative document entitled “Procedure for standardized testing of terrestrial laserscanners” by NEITZEL ET AL. (2013) which directly addresses the users rather than the scientists and will propose a workable (field) procedure.

Until now, many contributions to objective testing and calibration of TLS systems in laboratories can be found, where universities and colleges are involved as well as manufacturers, which also work together in forums and initiatives (e.g. the “Offenes Forum Terrestrisches Laserscanning”). A comprehensive scientific overview can be found in GORDON (2008). At present, amongst others, testing sites exist at the HCU Hamburg (LINDSTAEDT ET AL. 2012), HS Bochum (FELDMANN ET AL., 2011), HTW Dresden (WEHMANN, 2007) and i3Mainz (KERN, 2011). Maximum testing range at this sites is restricted to < 25-30 m resp. <70 m (HTW Dresden), though. While theory already is well developed, the practical implementation is limited by halls being big enough for permanent testing facilities. The geodetic laboratory at the Chair of Geodesy at the Technische Universität München, which is a member of the Society for Calibration of Geodetic Devices (SCGD, in German: GKGM) now also is implementing some of the suggestions in an own laboratory hall.

2 Existing concept of a TLS testing procedure

The actual draft of a guideline for testing of terrestrial laserscanners by KERN (2010) called “Testing procedure for acceptance and control of terrestrial laserscanner systems¹” substantiates and widens pre-work and suggestions especially by BÖHLER (2005) and HEISTER (2006). The basic principles used here are based on the German VDI/VDE-guideline 2634 Volume 2 „Optical 3D-measuring systems – Optical systems based on area scanning²” (VDI/VDE 2634, 2012) and are meant to introduce a consistent testing procedure based on selected, comprehensible and use-oriented specifications. The basic principle is the measurement of geometric and calibrated testing specimens of superior accuracy which become arranged spatially distributed in a well-defined measurement volume.

The measurements themselves have to be done under usual conditions. The determination of specifications is done using least-squares adjustment. To achieve a complete system test, data evaluation should be performed using the (manufacturers’) software bundles which are being used also in every-day’s work, but as some evaluation tools still are missing therein, actually some special testing software is used. The VDI/VDE guideline allows various (data) filtering and pre-processing, where each a set of constraints for individual specifications is used. The documentation of the filter type and pre-processing steps would be useful in that case, but very often these information is subject to manufacturers’ corporate secrets.

In KERN (2008) and HUXHAGEN ET AL. (2009) the adoption of the VDI/VDE specifications by HEISTER (2006) is explained in more detail and widened for the use with TLS. The specification numbers are determined objectively and therefore can act as good clues to compare real quality measures of scanners to the manufacturers’ data as well as to other scanners. Unfavorable is the necessity of special and very accurate testing specimens and of a testing site covering the whole scanner range. The suggested quality parameters are:

2.1 Probing error

The probing error R is defined as the standard deviation of all radial deviations r_i of n probing points which become used to estimate all the testing spheres with free radius in the testing volume. R is a parameter of the surface noise which is independent of the (varying) angle of incidence on the spheres’ surfaces. It is notably, that R is not equal to the line of sight noise and therefore the ranger precision. HUXHAGEN ET AL. (2009) goes into more detail when examining further dependencies on measurement distances and sphere size which become neglected here.

$$R = \sqrt{\frac{1}{n} \sum_{i=1}^n r_i^2} \quad (1)$$

¹ „Prüfrichtlinie zur Abnahme und Überwachung von Terrestrischen Laserscanner-Systemen“

² „Optische 3D-Messsysteme – Bildgebende Systeme mit flächenhafter Antastung“



Using the standard deviation s_{R_j} of the p estimated sphere radii, an additional accuracy statement can be given. In HEISTER (2006) the probing uncertainty u_R is defined:

$$u_R = \sqrt{\frac{\sum_{j=1}^p s_{R_j}^2}{p}} \quad (2)$$

2.2 Sphere-radius error

The sphere-radius error R_K is defined as mean value of all deviations of the k estimated radii compared to their known reference values. This parameter gives information on local systematic irregularities of form.

$$R_K = \frac{1}{k} \sum_{i=1}^k v_i \quad (3)$$

2.3 Sphere-spacing error

The sphere-spacing error ΔL is defined as mean value of all spacing deviations ΔL_j when the spheres have been estimated using a fix reference radius. The spacing deviations ΔL_j are derived from the known reference distances l_{kj} and the measured distances l_{mj} of p pairs of spheres. The reference distances have to be determined with superior accuracy in advance. The sphere-spacing error is a parameter of the TLS' size accuracy truth within its working volume.

$$\Delta L = \frac{1}{p} \sum_{j=1}^p \Delta L_j \quad \text{mit} \quad \Delta L_j = l_{kj} - l_{mj} \quad (4)$$

An additional accuracy statement is given by the standard deviation of the testing sample. In HEISTER (2006) the spacing uncertainty u_L is defined:

$$u_L = \sqrt{\frac{\sum_{j=1}^p \Delta L_j^2}{p}} \quad (5)$$

As an option the sphere-spacing error can also be obtained using 3D similarity transformations and taking the coordinates' standard deviations as point errors. However, when the scale factor is fixed to 1 (6-parameter transformation) while it significantly differs in reality, there might be a dependency between the sphere distances and the difference between measurement and reference values; for more details see KERN (2008).

2.4 Resolution power

The resolution power AV is defined as minimum joint width on a Böhler-star (BÖHLER, 2005), where points of a point cloud can significantly differed in front face points and back face points. Impact factors on AV are the sample rate (angle increments), beam divergence, angle of incidence, influences of signal processing and effective data filters, especially to improve surface noise. To see the mathematical definition, please refer to the literature mentioned above.

3 Practical TLS comparison series

The method of the Chair of Geodesy at the Technische Universität München described here is an objective comparison for TLS systems to evaluate accuracy, geometric truth, measurement speed and achievable range. It is meant as a contribution in objective TLS specification inquiry. The problem of the impact of scan quality settings on the resulting measurement noise and gross erroneous points at edges (signal interference) are of special interest. Generally we may assume that noise suppressing filters will yield good results on flat surfaces but we will lose geometry truth at edges. Calibrated test specimens will not be used in this approach.

Therefore a test procedure checklist was created which allows objective conclusions on different comparative parameters which are relevant in different tasks. As test specimens we intentionally use constructions which easily can be constructed and used by other interested people. Additionally, we use methods which are similar to the reference bodies tests and an examination of 3D accuracy which uses a testing site. However, the focus of this paper is laid on the simple methods which we chose in a way to cover the known scanners' ranges up to 200 m (in 10 m steps).

3.1 Scan quality settings

At first we need a little abstraction to be able to compare the impacts of all the various scan quality settings of different instrument types. Quality settings differ in names, but all mostly consist of different grades of raw data filtering f_{Dist} and a connected bandwidth of possible scan resolutions r . The impact of raw data filtering on the point clouds can only be evaluated empirically, as we do not know about the underlying algorithms. Their disclosure is not only an actual wish of engineering surveying specialist users, but also a necessity for real quality rating of measured point cloud data.

The comparison measurements performed are based on suitable quality settings with respect to the highest possible resolution setting. Then we make measurements at three settings: minimum quality (lowest setting, $f_{\text{Dist}} = 0\%$), maximum quality (highest setting, $f_{\text{Dist}} = 100\%$) and an intermediate setting ($f_{\text{Dist}} = 50\%$) where we define the latter to be the one which is the “recommended setting” by the manufacturers. Within each quality setting, we use the highest possible resolution $r = 100\%$ to get as many single measurement points on each target as possible.

3.2 TLS comparison conceptual design

A detailed overview on our concept can be found in Table 1. The comparison parameters mentioned therein will be shown in detail. Parts of the table which are highlighted in gray have not been executed in the context of our instrument tests, but are mentioned to complete our conceptual design.

3.3 Comparison parameter accuracy

When comparing accuracy, the ranger of the TLS system is getting analyzed. It is distinguished between measurement precision (statistical accuracy) and absolute 3D accuracy (correctness) of single, discrete points derived from 3D point clouds when using TLS targets.



Table 1: TLS comparison concept

Comparison attribute	Comparison parameter	Deduction	Realization	Testing parameter	Concrete values	
Accuracy	Precision	σ_{DIST} : ranger noise dependent on distance	Standard deviation of residuals of a free adjustment plane	Testing specimen: white surface with albedo and angle incidence testing fields, measurement distance in several intervals Δ_{DIST}	<ul style="list-style-type: none"> f_{DIST}: distance measurement filtering in [%] α: angle of incidence in [°] Albedo: reflection in [%] 	<ul style="list-style-type: none"> $\Delta_{\text{Albedo}} = \sim 40 \%$ $\Delta_{\alpha} = 15^{\circ}$ $\Delta_{f,\text{DIST}} = 50 \%$ $r = 100 \%$ $\Delta_{\text{DIST}} = 10 \text{ m}$
	3D-accuracy	$\sigma_{3\text{D}}$: absolute 3D accuracy <ul style="list-style-type: none"> σ_d: distance accuracy σ_{Hz}: horizontal angle accuracy σ_v: vertical angle accuracy Various calibration parameters	Result of a 3D network adjustment, LSA using redundant two-face measurement data	3D testing site using manufacturers' targets and software (system calibration)	none	$f_{\text{DIST}} = 0 \%$ $r = 100 \%$
Geometric truth	Edge behavior	n_{richtig} : geometrically correct points (geometrical truth with respect to distance)	Point classification using $3\sigma_{\text{DIST}}$ -confidence intervals	Testing specimen: White circular ring with defined distance from background, measurement distance in several intervals Δ_{DIST}	<ul style="list-style-type: none"> f_{DIST}: distance measurement filtering in [%] 	$\Delta_{\text{DIST}} = 20 \text{ m}$ $\gamma = 0^{\circ}$ $\Delta_{f,\text{DIST}} = 50 \%$
	Form truth	Geometric parameters (e.g. sphere radii)	Nominal/actual comparison of geometric parameters	Testing specimen: geometric reference body, measurement distance in several intervals Δ_{DIST}	<ul style="list-style-type: none"> $(f_{\text{DIST}}$: distance measurement filtering in [%]) 	$\Delta_{\text{DIST}} = 10 \text{ m}$ $(\Delta_{f,\text{DIST}} = 50 \%)$
Range	Maximum modelling range	d_{max} : maximum measurement distance to objects	Capture efficiency ϵ or proof of normally distributed measurements	Testing specimen: white surface, measurement distance in several intervals Δ_{DIST}	<ul style="list-style-type: none"> f_{DIST}: distance measurement filtering in [%] α: Angle of incidence in [°] Albedo: reflection in [%] 	$\Delta_{\text{DIST}} = 5\text{-}10 \text{ m}$ $\gamma = 0^{\circ}$ $\Delta_{f,\text{DIST}} = 50 \%$ $r = 100 \%$
	Maximum registration range	d_{ziel} : maximum measurement distance to targets	Nominal/actual comparison and quality of target coordinates	Testing specimen: manufacturers' targets, measurement distance in several intervals Δ_{DIST}	<ul style="list-style-type: none"> r: resolution setting in [°] $(f_{\text{DIST}}$ distance measurement filtering [%]) 	$\Delta_{\text{DIST}} = 5\text{-}10 \text{ m}$ $\Delta_{f,\text{DIST}} = 50 \%$
Speed	Time of data acquisition	t_{typisch} : typical measurement time [min]	Measurement time	Time measurement / data from handbooks	none	$f_{\text{DIST}} = 50 \%$ $r = \text{constant}$

3.3.1 Precision (Noise)

A measure for the precision of individual measurements of a TLS system is the deviation of measurements from a sample's mean value. The standard deviation of a LSA plane is defined as a reference value for single measurement noise. As the testing plane is set up perpendicular to the scanners' line of sight, influences of the angle of incidence can either be neglected or specially be analyzed by a defined tilt of the plane. The determination of the precision is done similar to the probing error concept of HEISTER (2006) and HUXHAGEN ET AL. (2009).

Our testing specimen is a 60 cm x 80 cm flake board which has been coated with a dim white and therefore is diffusively dispersive surface. It is furthermore subdivided in individual testing areas for special testing parameters (Fig. 1). The areas at the left and right are used to determine σ_{DIST} relative to the measurement distance (precision of the ranger) when the specimen is scanned in constant intervals within the full scanner working range. To simulate different material reflection, customary photographic gray value cards are attached in the center (Opteka gray cards, black RGB 16/16/15, gray RGB 162/162/160 and white RGB 220/224/223). The albedo values of these cards have been determined in the Leica laboratory in Heerbrugg as completely diffuse reflection with 5% uncertainty, while the albedo is defined as the reflective value determined compared to an "ideal" diffuse reflector.

The albedo values are dependent on the laser's wave length. In table 2 the wave lengths of the Leica scanners HDS7000 and Scanstation P20 are listed. The Faro Focus^{3D} which was not tested for albedo values uses a 905 nm laser.

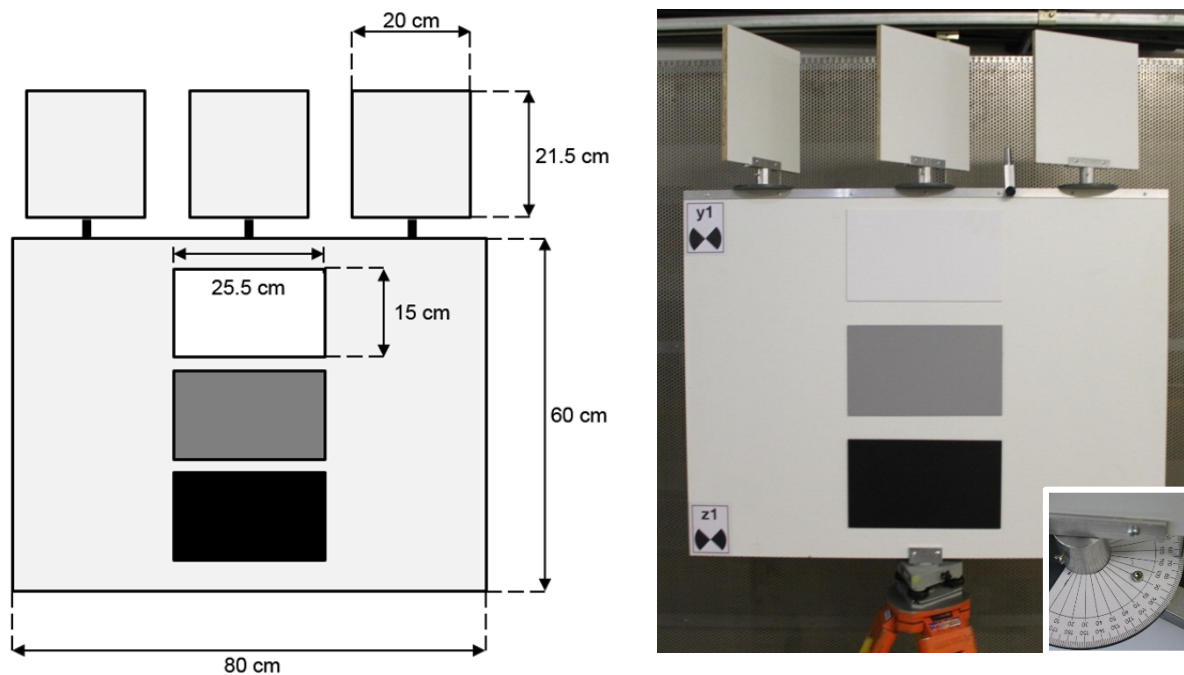


Figure 1: Specimen "Board" to determine TLS noise

**Table 2:** Albedo-values of testing areas

Testing area	Albedo values for tested wave lengths	
	Leica HDS7000 (1550 nm)	Leica ScanStation P20 (808 nm)
White coated flake board	53,6%	87,5%
White gray value card	83,1%	86,3%
Gray gray value card	33,2%	32,5%
Black gray value card	5,2%	5,8%

On top of the board three vertically rotatable testing planes identical to the board material are mounted to simulate different angles of incidence (see fig. 1 down right). The combination of so many individual testing areas is used to obtain a broad spectrum of different testing cases (parameter sets) out of one single scan and therefore under identical circumstances. Doing so, we get a direct comparability of different object characteristics and save lots of testing time. For individual testing, the combination of the areas may be chosen on anyone's demands.

3.3.2 3D Accuracy

The 3D accuracy is an absolute accuracy value and defined as the mean deviation of measured coordinates from their reference values. To determine them, coordinates from high-definition TLS target scans are used which are calculated using LSA with very high redundancy and therefore are virtually free from ranger noise effects. The 3D coordinate's accuracy can be expressed either by the point error σ_{3D} or by the repatriated standard deviations σ_d (distance), σ_{Hz} and σ_v (angles). Influencing parameters are all (systematic) errors in distance measurement (e.g. additive and scale constants), imprecision of the angle measurements as well as axis errors and eccentricities. KERN ET AL (2008) give a compilation and classification of all possible influencing parameters.

In a current master's thesis (REIDL, 2012) at the Chair of Geodesy of the Technische Universität München, an approach from NEITZEL (2006) is used and extended to determine TLS axis errors; the possibility of a measurement in two faces is required for this. The advantage is, that known reference values are unnecessary by using a 3D point field. NEITZEL (2006) performs a pure component calibration while REIDL (2012) extends this in terms of a system calibration and uses the laserscanner's dedicated targets and analyzing software. The additional influences of the overall system are reflected in the observations' accuracies of a free 3D network adjustment (LSA). These are considered in the calibration, whereby the system reference is established. Besides the axis errors, also other instrument errors (e.g. vertical collimation error) can be determined within the 3D network adjustment. This is an extension of HESSE (2008).

Furthermore current studies deal with the determination and separation of additive and scale constant. First results show erratic influences, depending on the distance, and therefore a non-linear scale factor, which indicates a piecewise correction with Lookup-Tables.

3.4 Comparison parameter geometric truth

We defined the term “geometric truth” during this TLS comparison series especially to examine the impact of (smoothing) filters on the point cloud quality. Here we consider the share of geometrically erroneous points to be of special interest. Furthermore it can be analyzed, whether an explicitly defined geometric body is really represented by the measured point cloud in geometry and size.

3.4.1 Edge behavior

Especially at clear geometric edges or at nose faces (i.e. parallel levels with different depth), false points created by interference reflections arise (e.g. the so-called comet-tail effect). Although ToF scanners use full-waveform-analysis which may reduce such a worsening (WEHMANN ET AL., 2007), smearing effects can be found at edges. In practical work, edge modelling hence is only done using plane intersection while neglecting measurements in the edges’ surroundings. If the data for plane adjustment is worse or even missing (emersed objects or due to shadowing effects), the true object boundaries can no longer be obtained. This problem is intensified by raw data filtering, because this may lead to broader areas of interference signals. In addition, systematic patterns and artefacts can be found at edges. The reason for that (see fig. 2) is subject for further investigation, but shall be at least mentioned here.

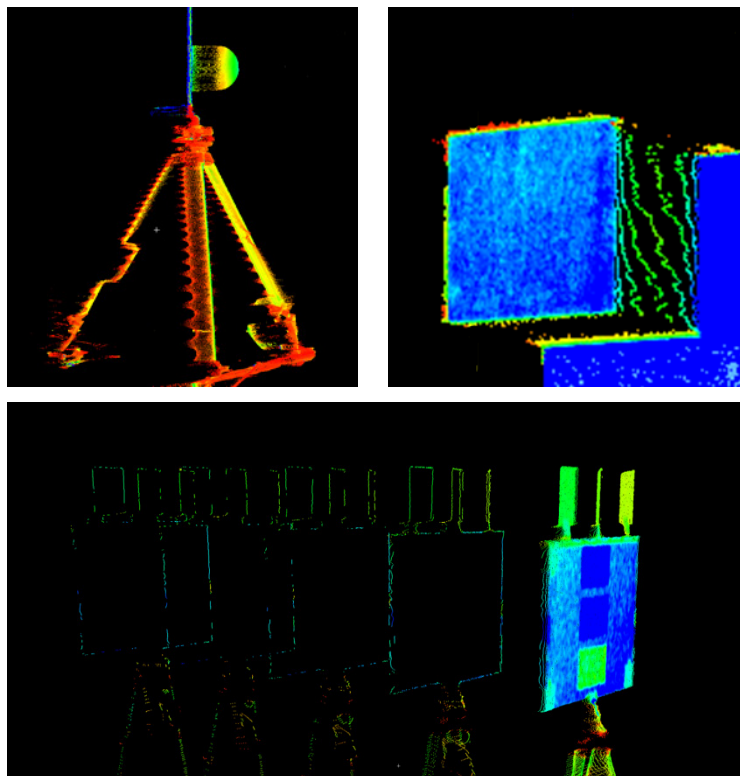


Figure 2: Erroneous points when scanning edges (HDS7000): Sphere mounted on plane on tripod (top left) with interference points and artefacts at tripod legs, vertical edge with interference points (top right) and object silhouettes misplaced backwards (down)

In all day’s work the determination of object boundaries (edges) is an important task. Ranger precision (point cloud noise ratio) is not the critical thing here – in fact misplaced points is much more problematic for modelling. Thus we examine the impact of scan quality settings on the geometric truth concerning edge detection here: the “geometric truth” $n_{\text{richtig}} [\%]$ is the per-



centage of scanned points which are suitable to characterize a given geometric specimen correctly, i.e. not influenced by interference signals. Mathematically we define those points to be correct, which are contained in a $\pm 3\sigma_{\text{DIST}}$ confidence interval around the reference geometry (1% error probability), where σ_{DIST} is the empirical standard deviation of a LSA geometry and is thus based on the individual noise level of the scanner in use. As the result value is a percentage, this comparison value is theoretically independent of the chosen resolution.

As a specimen a breaker plate with a 10 cm wide ring is used which is mounted 10 cm in front of a white 60 cm x 60 cm background plane (fig. 3). To allow exact edges in measurement direction, the lateral planes have been beveled towards the backside, so no laser signal can strike there. Both the “board” and the “breaker plate” have been crafted in the geodetic laboratory’s precision mechanical workshop. The testing concept shown here widens the suggestions for edge detection, which were made by BÖHLER (2005) and WEHMANN ET AL. (2007) in a merely qualitative way. It may be adopted and expanded to any desired geometry.

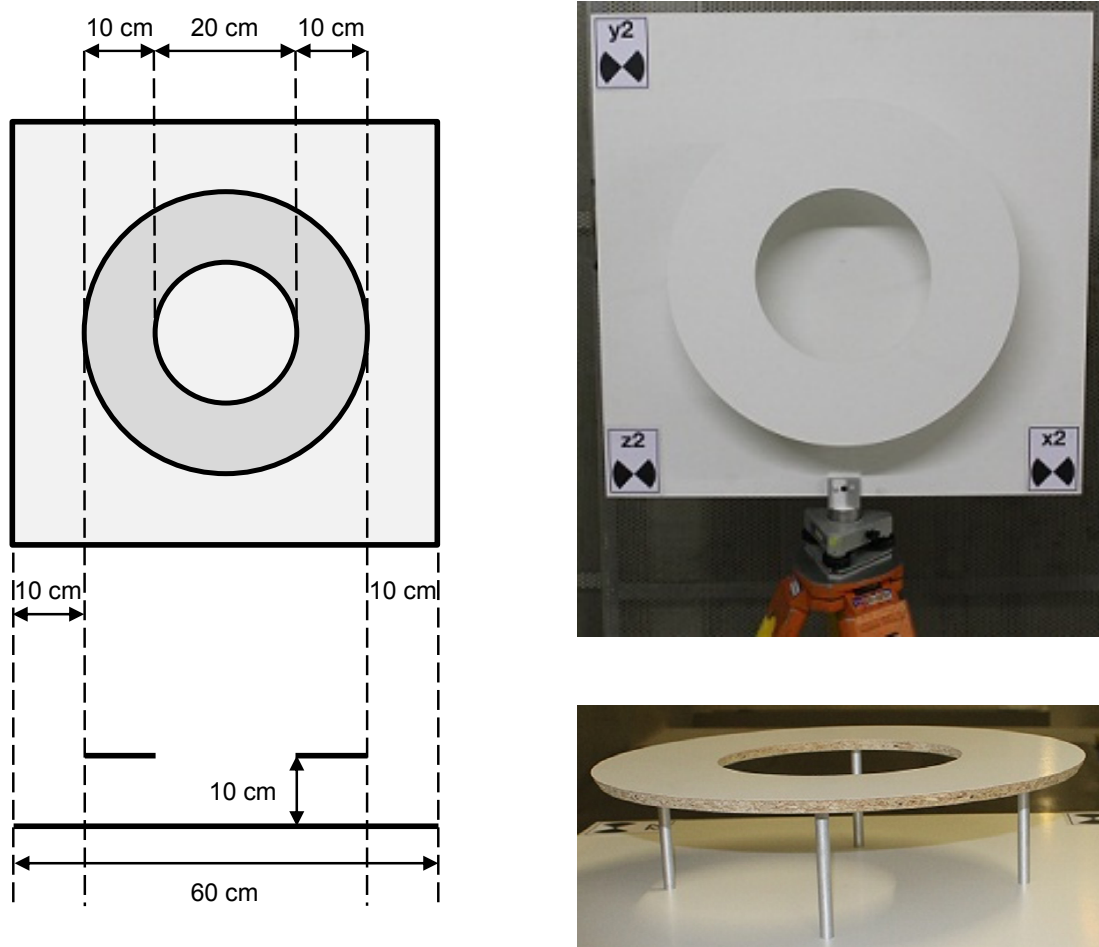


Figure 3: Specimen „Braker plate“ to determine a TLS' edge behavior

We intentionally do not used a fixed bandwidth for evaluation (e.g. some centimeters), as our threshold complies with the usual definition of gross errors in geodetic observations on the one hand, and is also similar to the typical modelling process using LSA and geometric primitives on the other. Higher scan quality influences point cloud quality, especially by reducing noise. Hence, for the user the point cloud seems to be more precise; but this will probably lead to a higher rate of geometric false points as described above. To increase point cloud

precision (or to reduce single point noise) does therefore not mean a better geometric truth – it may even degrade. So the comparison parameter n_{richtig} is not to be thought of being dependent from the noise level σ_{DIST} – our concept acts more like a normalization towards the scanner's noise level which allows the result to be comparable.

Continuative considerations on TLS resolution quality are not performed here. Please refer to the relevant literature, especially the tests of BÖHLER (2005).

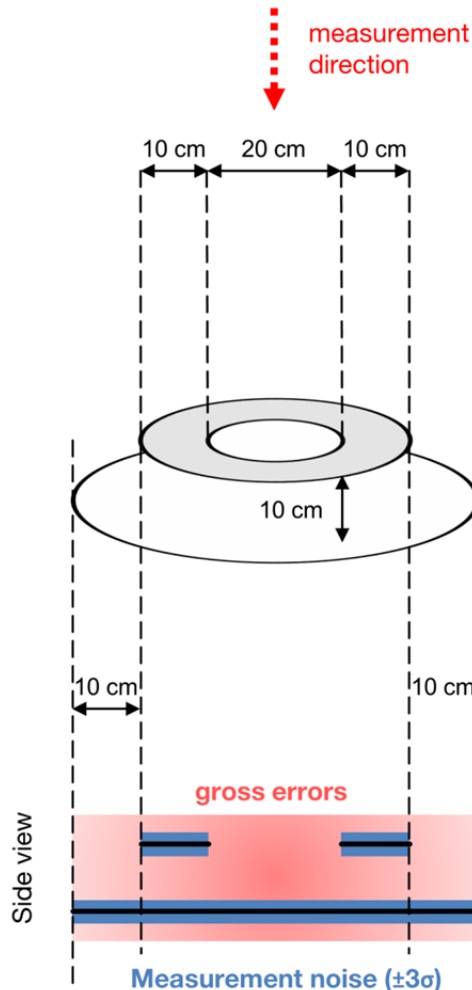


Figure 4: Determination of the comparison parameter n_{richtig} to rate the edge behavior

3.4.2 Form truth

To measure form truth usually the sphere-radius error R_K is used (see formula 3). By different radii R in adjusting LSA spheres, a mean value of the relative equivalence of the determined R and the reference values can be found. It gives information about the geometric quality of derived objects, and thus about modelling quality. As point number usually is high redundant, noise effects may be neglected. To use a sphere as a specimen is especially suitable, as it allows varying angles of incidence and different reflection intensities over the full possible ranges.



When modelling, it is necessary to identify those points which will really be used for the best-fit algorithm. Usually all points, which occur because of interfering signals and thus are erroneous (comet tail effect), become disregarded. This also implies, that geometric and size truth cannot be found for the measurement data, but only for the result of a special modelling algorithm.

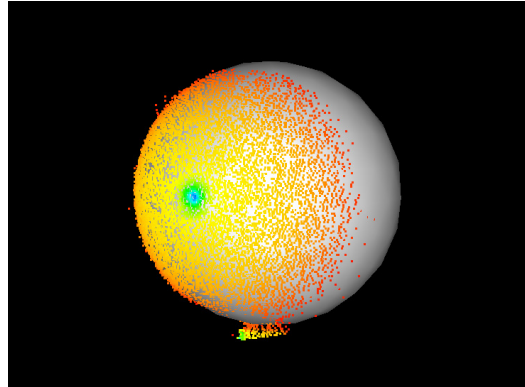


Figure 5: Best-fit sphere out of point cloud (TLS-System HDS7000)

Apart from spheres, from truth can also be derived with other geometric primitives, e.g. intersection angles of best-fit planes or area or capacity values of reference bodies.

3.5 Effective working range

Within the range values stated by the manufacturers one might expect results of different quality, dependent on beam divergence, angular resolution, ranger quality and target surface. This impacts point density as well as usability of an individual point.

3.5.1 Maximum modelling range (object measurement)

The capture efficiency $\varepsilon(d)$ is calculated as the ratio between theoretical and real number of measurement points on an object with respect to the measurement distance d (see fig. 6). A criterion for a maximum possible range which is suitable for practical work is a minimum allowable value ε_K (pre-defined critical capture efficiency).

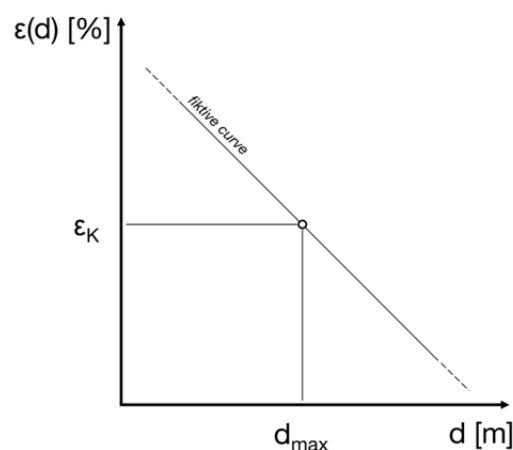


Figure 6: Maximum modelling range and critical capture efficiency

The determination of the maximum modelling range d_{\max} thus can be done (assuming a linear relation) by:

$$d_{\max} \text{ at } \varepsilon(d_{\max}) = \varepsilon_K \text{ and } \varepsilon(d) = \frac{n_g(d)}{n_t(d)} \quad (6)$$

The number of theoretical points n_t on a testing plane is calculated by the given measurement distance d and the angular resolution. The number of points being really available is obtained by counting points inside a $\pm 3\sigma_{\text{DIST}}$ confidence interval of the LSA plane. The minimum allowable value ε_K needs to be chosen sensible. A recommendation is dependent on the later use of the data. In addition the residuals of the measurements after the LSA can be analyzed regarding their affiliation of a normal distribution. This is equal to a reliability measure for single points in a given distance and allows to detect a suitable maximum distance for reliable object modelling.

As a testing specimen one may use a plane or sphere, where possible influences of angle incidence and reflectivity should be regarded. Testing is done on a linear track with at least the length of the nominal working range of the scanner. It may usefully be combined with the determination of the noise σ_{DIST} .

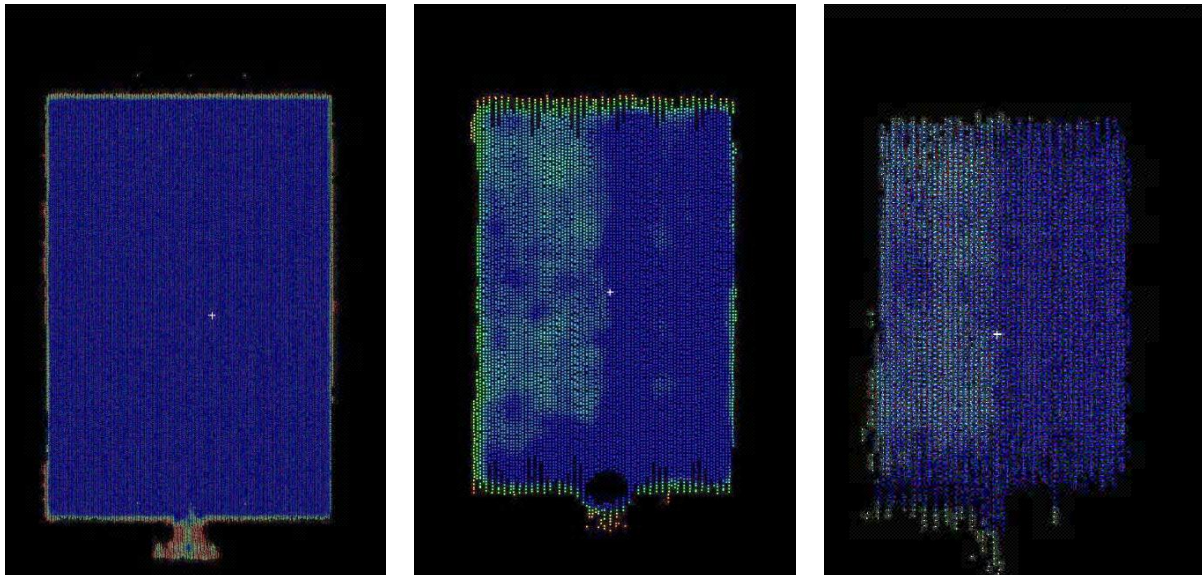


Figure 7: Capture efficiency on a white plane surface at 20 m, 100 m and 160 m distance (HDS7000)

3.5.2 Maximum registration range (target measurement)

Comparison tests in range are also to be performed for target modelling. This allows information on the usability of manufacturers' targets for data registration dependent on the measurement distance, which might significantly differ from object modelling distance. A general determination concept and a concrete guideline for the HDS7000 is currently in progress at the Chair of Geodesy at the Technische Universität München.

On the one hand we need to detect the quality of the geometric modelling and target point calculation with the points available in a certain distance at all, on the other hand it is necessary to verify them with reference values. Suitable limits need to be defined to ensure a desired registration accuracy. The examination needs to consider (predefined) resolution settings and scan quality settings. If a (usually too short) comparator track is available, scale irregulari-



ties can be uncovered in addition. For full range scale examination, long reference tracks become necessary.

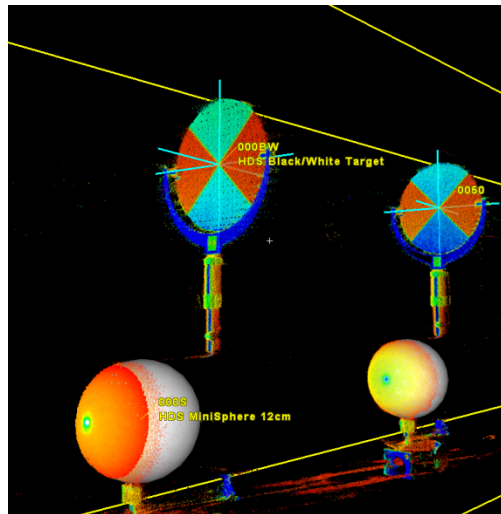


Figure 8: Analysis of measurement distance using different targets (HDS7000)

3.6 Measurement speed

Determination of data acquisition speed is rather trivial. We use a panorama scan with 5 mm point resolution at 10 m distance and a medium scan quality setting, which gives us a typical measurement time t_{typisch} . Predefined resolution settings may differ from that; therefore with many predefined quality and resolution settings an impartial comparison is only possible with limitations.

Of special interest is the fact, whether higher quality settings with significantly longer measurement times are justifiable by an accuracy gain. This can be done in combination with all the comparison methods mentioned above, and is to be performed best in the context of a real business task.

4 TLS systems compared (scanners and software)

To get practical results of our comparison concept, three scanners sold by Leica Geosystems and Faro have been used: the Leica HDS7000 (identical in construction to the Zoller & Fröhlich Imager 5010) and the Faro Focus^{3D} which use the phase comparison principle (PCP) as well as the Leica ScanStation P20 which is a time-of-flight instrument using Waveform Digitizing (WFD). WFD may be thought of a combination of PCP and ToF – theoretically a high measurement speed can be combined with high accuracy in medium working range.

To see the specifications of the manufacturers' data sheets, especially regarding the nominal distance uncertainty, please refer to the appendix.



Figure 9: From left to right: TLS systems Faro Focus^{3D} (FARO 2013), Leica HDS7000 (LEICA, 2013) and Leica ScanStation P20 (LEICA, 2013)

4.1 Data conversion and import filter settings

In the TLS testing series described in the following, data conversion was done using the manufacturers' original software Leica Cyclone (Version 7.4.1) and Faro Scene (Version 4.8). Data conversion for the HDS7000 point clouds in *.zfs format were done with Leica Cyclone using preset standards³. Measurement data of the Focus^{3D} also have been processed using the Faro Scene standard settings⁴. The ScanStation P20 data conversion had to be done with a prototype software tool "DataCopyTool" outputting *.ptg format files to be used with Cyclone then. The prototype software was provided by Leica, because Cyclone 7.4.1 was not able to access P20 data at testing time as that scanner was still under development. During conversion to *.ptg format also the standard settings were used⁵.

³ Software menu *Edit* → *Phase-Based Scanner Filter Settings* → *Filter Setting For: HDS7000* → *Intensity: Minimum 0.06 Maximum 120 %*, *Invalid (Skirt): Angle 25 deg*, *Mixed Pixel: Pixel 6 Angle 2 deg*, *Range: From 0.5 To 187 m*, *Single Filter: Pixel 2*, *Intensity Overload Threshold: 5718750*

⁴ Software menu *Tools* → *Options* → *Default Filter* → *Apply default filter on first load: Yes*, *Reflectance Threshold: 300*, *Grid Size: 3 px*, *Distance Threshold: 0.02 m*, *Allocation Threshold: 50 %*

⁵ Software menu *Export Scan* → *Filtered PTG Format (*.ptg)*



To judge the impact of the import filters on the results of noise and edge behavior, all the analyses have been done with deactivated filter settings in a second run also. Filter deactivation is possible in the software menu settings. It is important to understand the difference between import filtering and scan quality settings (which also are filters), because the latter are already applied at data capture time and cannot be avoided, while the first only affect at import level (see fig. 10).

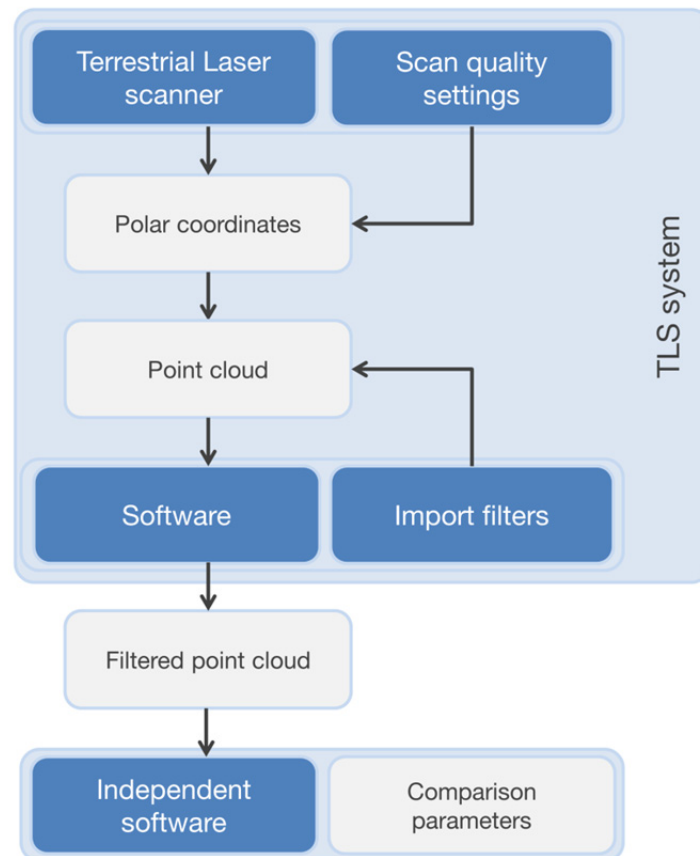


Fig 10: Testing scheme and distinct definitions

All the survey thereafter and the determination of the comparison parameters were made using a manufacturer-independent in-house software. Regarding these steps, one can speak of a TLS system test.

4.2 Tested scan quality settings

In the tests comparable settings within the predefined quality classes have been used. Out of all settings available, three most representative have been chosen and defined in percentage for the effective distance filtering f_{DIST} .

- $f_{\text{DIST}} = 0 \%$: lowest quality setting
- $f_{\text{DIST}} = 50 \%$: medium / recommended setting
- $f_{\text{DIST}} = 100 \%$: best quality setting

Within the quality settings the highest possible resolution setting $r = 100 \%$ was used (when $f_{\text{DIST}} = 100\%$ usually the possible resolution setting is comparably low):

Table 3: Scan quality settings f_{DIST} and highest possible resolution $r = 100\%$

TLS-System	$f_{\text{DIST}} = 0\%$	$f_{\text{DIST}} = 50\%$	$f_{\text{DIST}} = 100\%$
Focus ^{3D}	„1x“	„4x“	„8x“
HDS7000	„Low quality“	„Normal quality“	„Premium quality“
ScanStation P20	„1“	„2“	„4“
	$r = 100\%$ for scan quality f_{DIST}		
Focus ^{3D}	„1.538 mm/10 m“	„1.538 mm/10 m“	„6.136 mm/10 m“
HDS7000	„Super High“ (3,1 mm/10 m)	„Extreme High“ (0,6 mm/10m)	„Ultra High“ (1,6 mm/10 m)
ScanStation P20	„1 mm/10 m“	„1 mm/10 m“	„2 mm/10 m“

4.3 TLS testing track Eichenau

At the outdoor testing site of the Max Kneißl institute (MKI) of the Chair in Eichenau a 180 m track with marked setup points in 10 m intervals was realized. All measurements were performed on three subsequent days in August 2012 when weather conditions were sunny and calm. The scanners and the testing specimen have completely been shaded and were not exposed to direct sunlight.

To guarantee best comparability, all scanners have been set up on a baseline perpendicular to the measurement direction and with identical sighting axis height (fig. 11). From the same setup line, a tacheometer was used to adjust the instrument heights (using housing markers) and to align the specimens. As the Focus^{3D} does not have a sighting axis marker, the rotation mirror was assumed as height reference. The specimen centers were adjusted to the same height and their plane normals have been parallel to the sighting axes. To achieve this, the reflectorless tacheometer was used when targeting at small dim coated black & white targets (see fig. 1 and 3).



Figure 11: Instrument setup at TLS testing track

4.4 TLS testing field Munich

REIDL (2012) designed a TLS testing field for determination of TLS systems' exterior accuracy and installed it in a building of the Technische Universität München (Figure 12). The whole building is very good accessible, which allows a good spatial distribution of the TLS targets and instrument viewpoints.



Figure 12: TLS testing field (left), installation of the targets (right)

Twelve targets are installed with tapped holes in the structural steelwork, which allows the usage of several proprietary targets (Figure 13). Five viewpoints are implemented by means of three tripod points and two wall brackets. The maximum target height is 10 m, the maximum target distance 29 m.

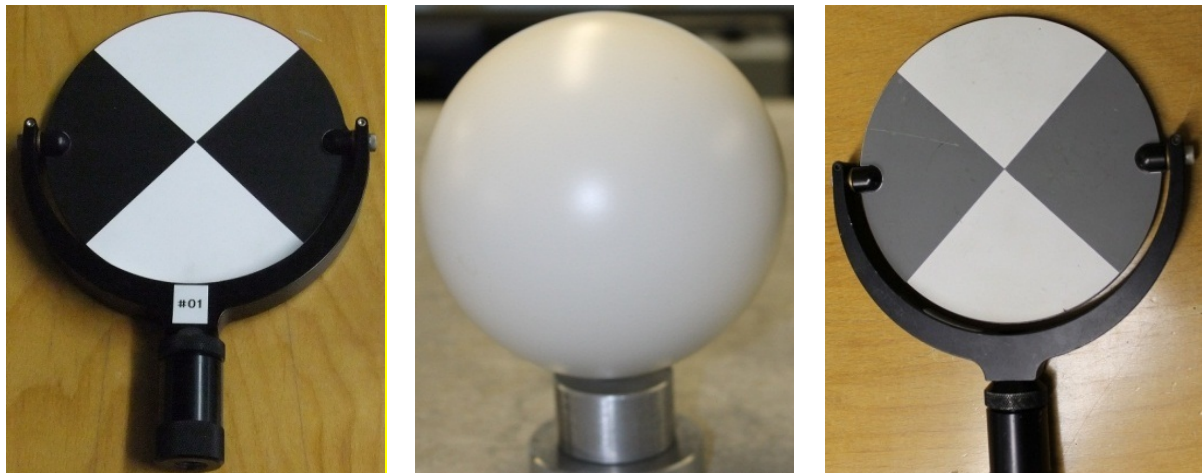


Figure 13: Proprietary and recommended TLS targets, from left to right: Leica HDS7000 Black/White-Target, Faro Focus^{3D} Sphere und Leica ScanStation P20 Gray/White-Target

The Black/White- and Gray/White-Targets are so called ‘Tilt and Turn’-Targets, which accordingly can be aligned towards the viewpoints. Studies at the geodetic laboratory showed a mean error of 1.5 mm (0.5 mm to 2.4 mm range) for these type of targets, which consists of a tumble error in the rotation axis and an error in the pivoting axis. This should be considered for high accuracy applications.

4.5 Precision (noise)

For the noise analysis an independent in-house software kit was used. The automatic evaluation of the measurement series is fully based on the ASCII point cloud data in various measurement distances, which are available via data export routines from the standard software. A integrated documentation of the quality of the adjusted comparison parameters is included (especially regarding the frequency distribution of the residuals).

To detect the distance-dependent noise σ_{DIST} of the ranger, the standard deviation of the residuals of LSA planes in the individual testing areas of the “Board” specimen have been evaluated for each 10 m. The segmentation is done automatically resulting in the testing areas which can be seen in fig. 14:

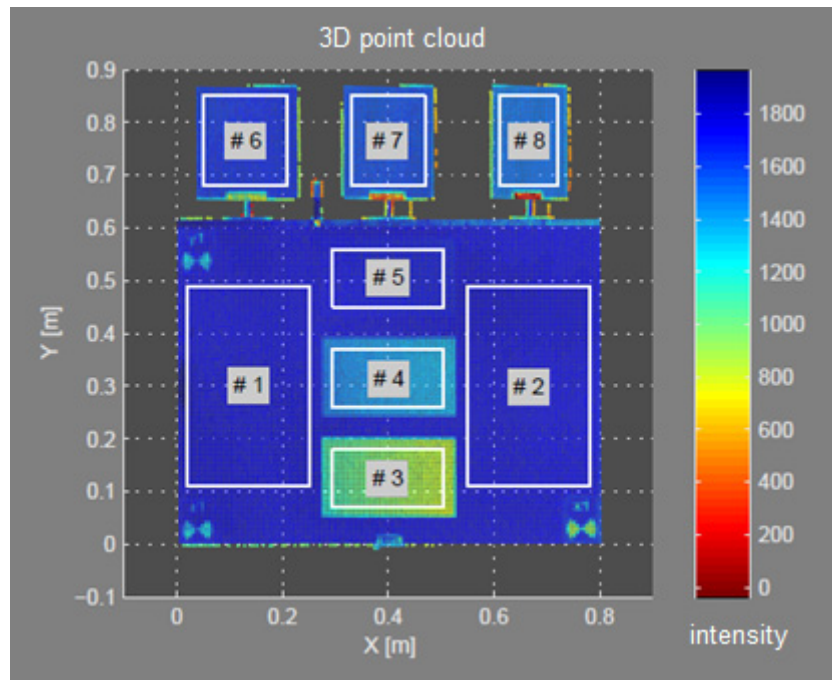


Figure 14: Segmented testing areas for different reflective levels and angles of incidence

All noise values have been determined with the three scan quality levels mentioned above to detect the scan filter setting influence. The results are shown with standard import filter settings and without any import filter.

- Noise $\sigma_{DIST,w}$ at white area (#1)
- Noise $\sigma_{DIST,g}$ at gray area (#4)
- Noise $\sigma_{DIST,s}$ at black area (#3)
- Noise $\sigma_{DIST,45}$ at white area, tilted by 45° (#8)

The noise at the areas tilted by 15° and 30° expectably showed results in between $\sigma_{DIST,w}$ and $\sigma_{DIST,45}$. The $\sigma_{DIST,45}$ result was reduced to the measurement direction component, while the relation between the angle of incidence α , the standard deviation σ_{res} of the residuals of the LSA plane and the resulting noise σ_{DIST} parallel to the laser beam is regarded as

$$\sigma_{DIST} = \frac{\sigma_{res}}{\cos\alpha} \quad (7)$$

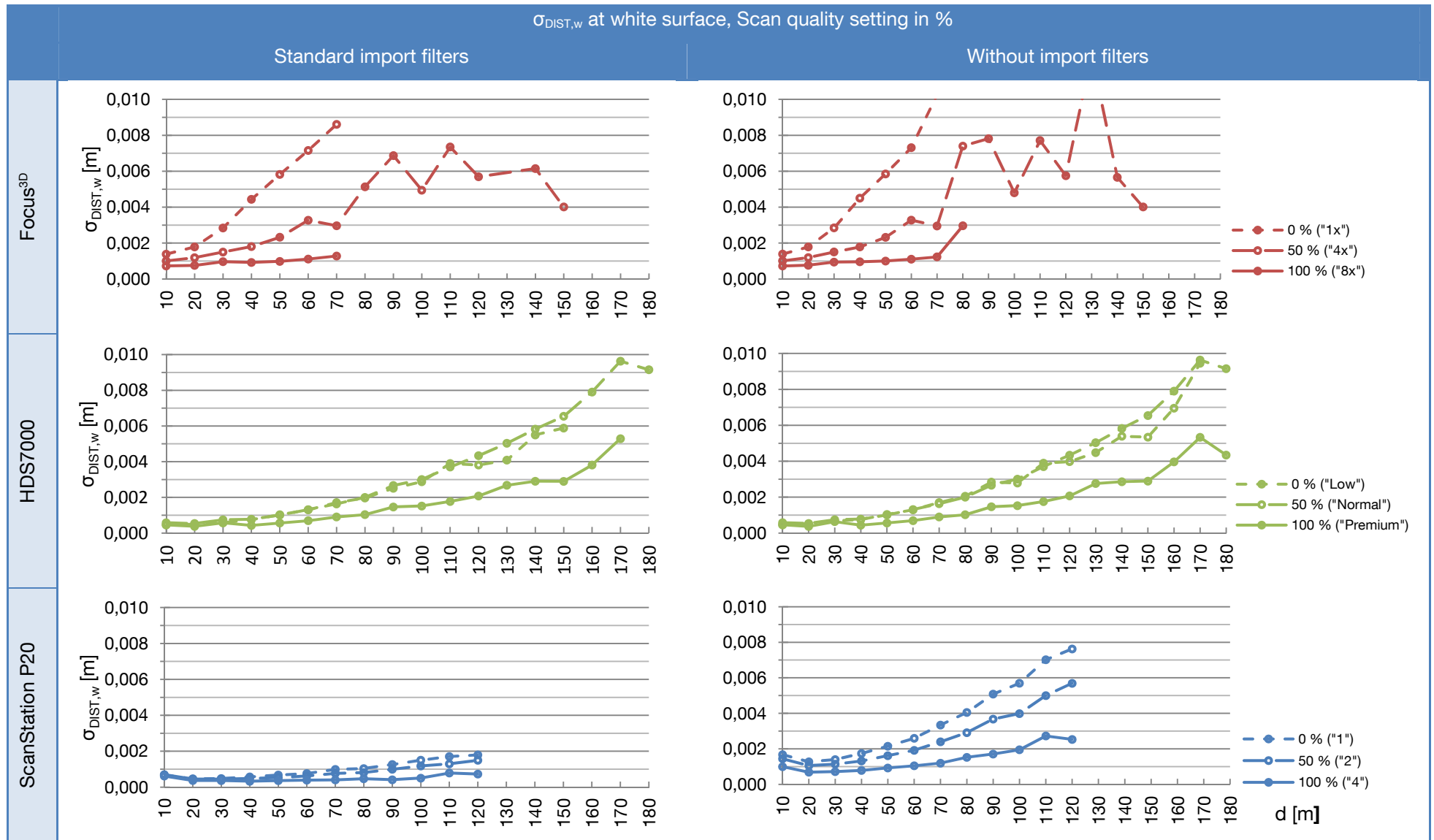


Figure 15: Noise $\sigma_{\text{DIST},w}$ at white surface

Objective Specifications of Terrestrial Laserscanners

Th. Wunderlich, P. Wasmeier, J. Ohlmann-Lauber, Th. Schäfer, F. Reidl

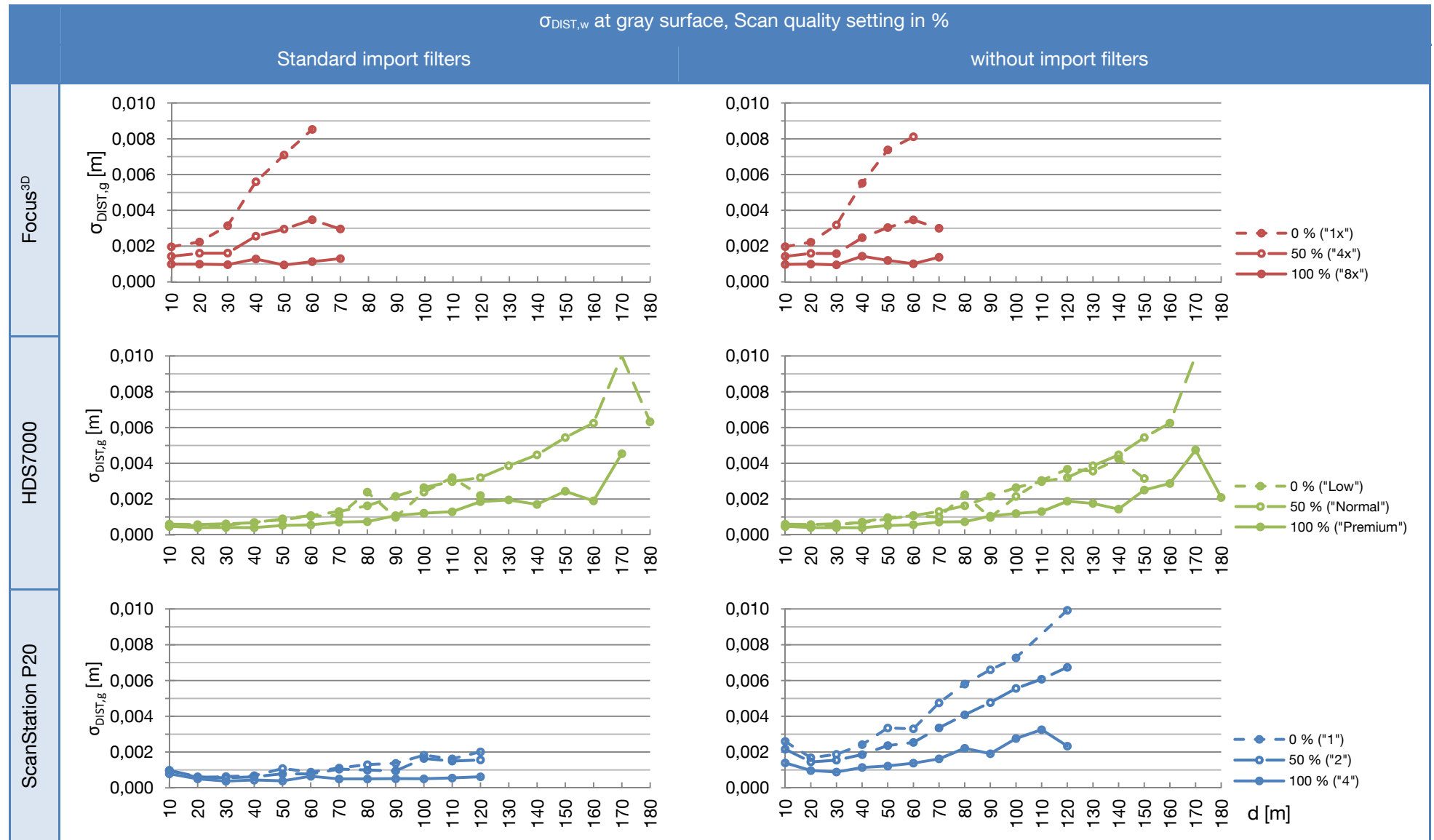


Figure 16: Noise $\sigma_{\text{DIST},w}$ at gray surface

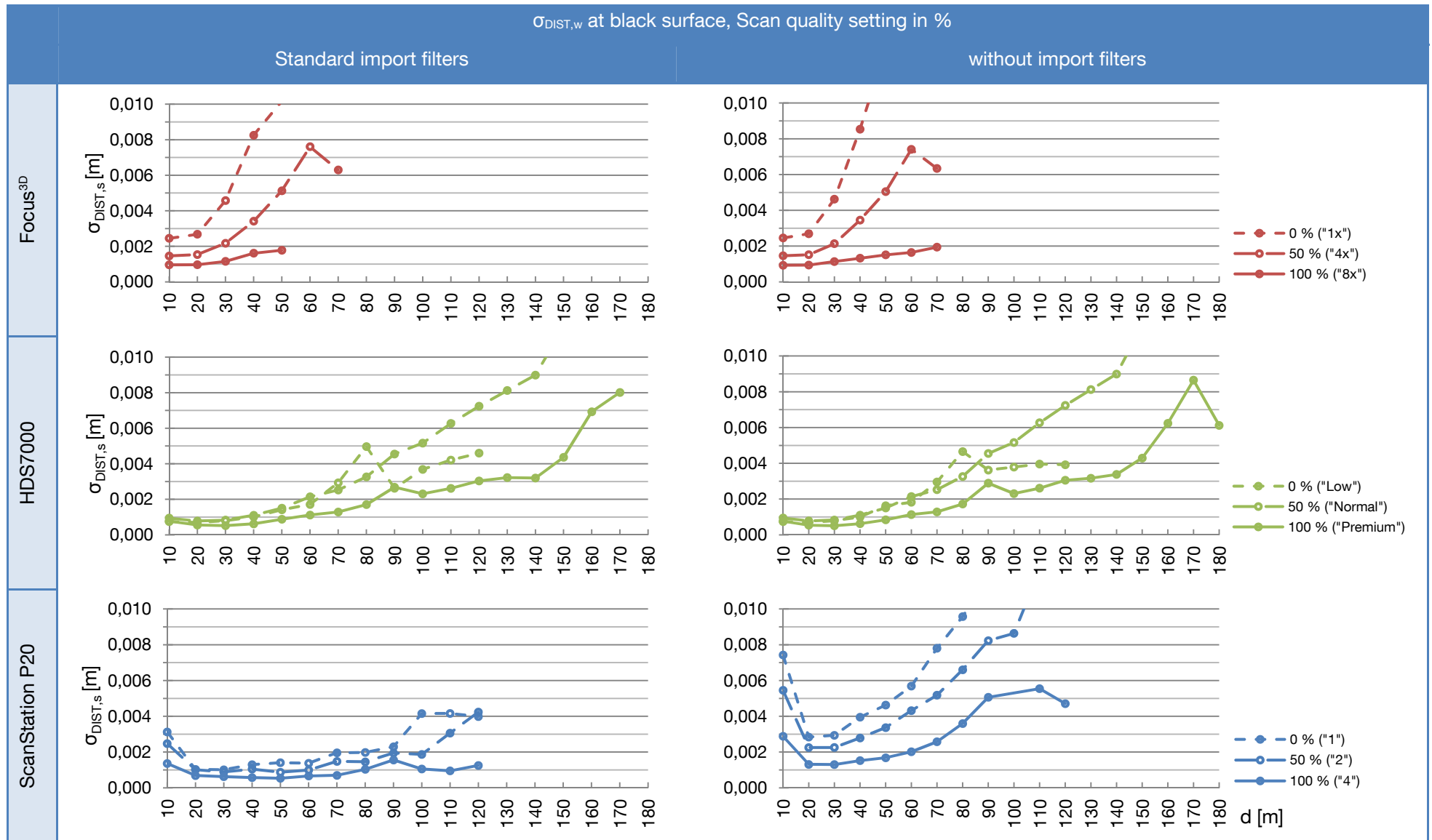


Figure 17: Noise $\sigma_{\text{DIST},w}$ at black surface

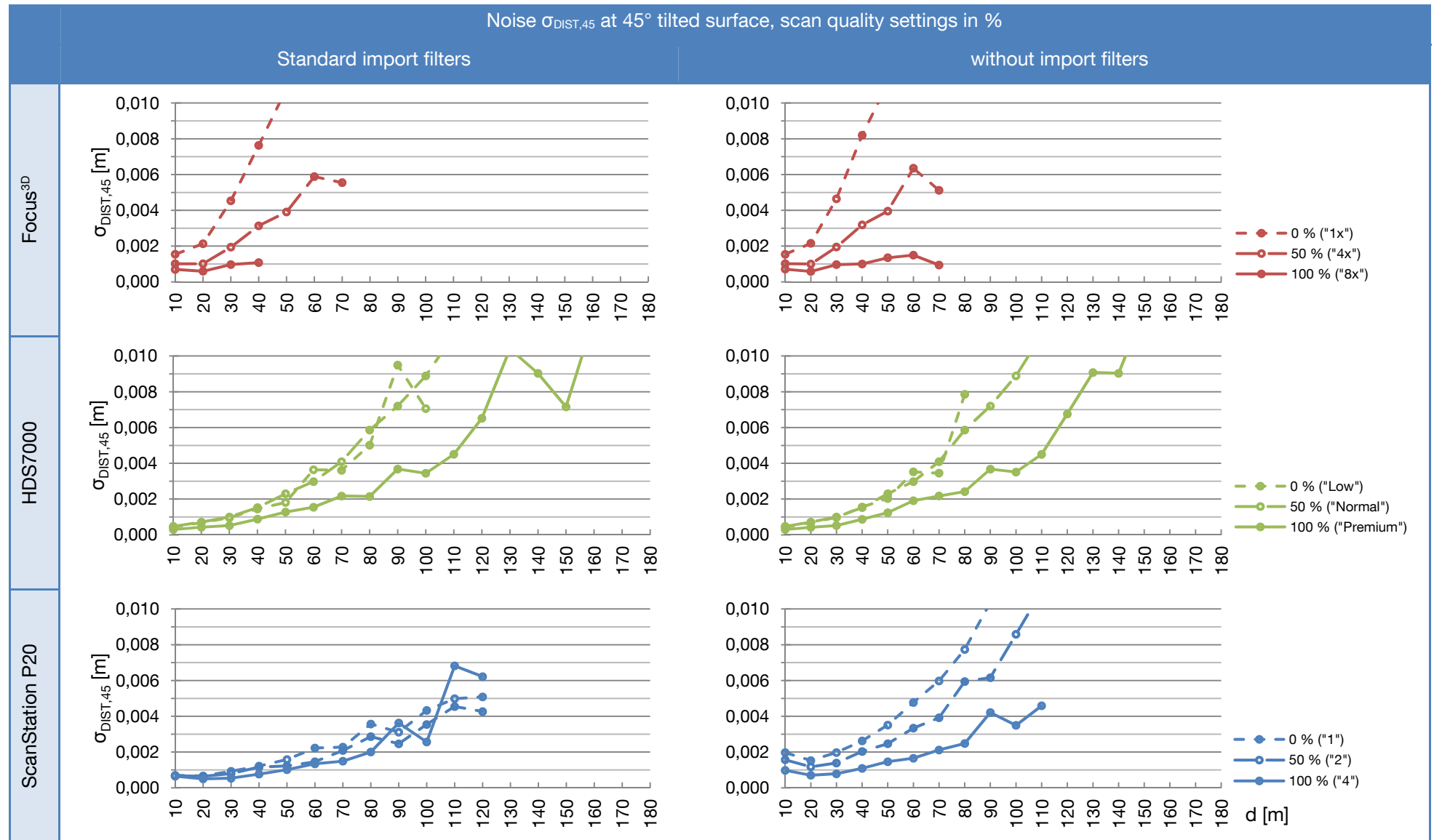


Figure 18: Noise $\sigma_{DIST,45}$ at white, 45° tilted surface

4.6 3D accuracy

With all three TLS systems 10 targets were scanned from 5 viewpoints in the described TLS test field (4.4) and analyzed with the respectively proprietary software. The target coordinates in the scanners' local Cartesian systems can be recalculated into polar values (d, H_z, V). The redundant observations allow statements about the observations' accuracy, using a 3D network adjustment. Again, additive constant and scale can't be determined without further information. However the result can be equaled to the registry accuracy as given in TLS analyzing software. The observations' mean accuracies, which were calculated with the geodetic software Cremer Caplan (CREMER, 2013), are listed in table 4, cf. REIDL (2012). Caplan's outputs by default are the standard deviations in position ($\sigma_{x/y}$) and height (σ_z), the variances of the polar values are derived with error propagation.

Table 4: Mean accuracy of the recalculated polar values

TLS system	σ_d [mm]	σ_{H_z} [mgon]	σ_V [mgon]	$\sigma_{x/y}$ [mm]	σ_z [mm]
Focus ^{3D}	±1.9	±9.6	±10.9	±0.9	±0.8
HDS7000	±1.8	±4.7	±11.7	±0.6	±0.8
ScanStation P20	±0.9	±2.8	±3.8	±0.3	±0.2

To ensure an objective comparison, the same network configuration was used for the three scanners. Also enough warm-up time was applied (about 30 minutes), whereat the tests showed the Faro Focus^{3D} needing even more time for a steady measurement accuracy.

4.7 Calibration parameters

Furthermore TLS measurements were performed in two faces in the test field, to determine the sighting axis error i , horizontal axis error c , eccentricity of the sighting axis e and vertical collimation error f_h , according to NEITZEL (2006); additionally their statistical significance can be tested. NEITZEL (2006) requires laboratory conditions and therefore assumes that observations are uncorrelated und have the same accuracy. Since the overall system was used under practical conditions, that assumption isn't permitted in this work. Instead the observations' covariance matrix of a free 3D network adjustment is used as cofactor matrix in the estimation of the instrumental errors, cf. REIDL (2012). The significance of the errors is proved with a concluding t-Test.

Table 5 shows the calibration's results for the systems Leica HDS7000 and Leica ScanStation P20. Unfortunately the Faro Focus^{3D} isn't able to perform scans in two faces, which is why this approach can't be applied for this scanner.



Table 5: Calibration parameters

TLS system	Sighting axis error			Horizontal axis error		
	i [mgon]	σ_i [mgon]	significance	c [mgon]	σ_c [mgon]	significance
HDS7000	-0,51	$\pm 0,44$	no	11,99	$\pm 0,48$	yes
ScanStation P20	-0,63	$\pm 0,33$	no	4,20	$\pm 0,43$	yes
TLS system	Eccentricity of the sighting axis			Vertical collimation error		
	e [mm]	σ_e [mm]	Signifikanz	f_v [mgon]	σ_{f_v} [mgon]	Signifikanz
HDS7000	0,06	$\pm 0,08$	no	-4,47	$\pm 0,53$	yes
ScanStation P20	0,01	$\pm 0,06$	no	1,24	$\pm 0,24$	yes

Particularly the significant horizontal axis errors and vertical collimation errors are to be mentioned. In REIDL (2012) concluding examinations are performed regarding a minimal configuration for the test field as well as the instrumental errors' effects on geometric parameters, modeled from a scanner's point cloud.

4.8 Edge behavior

The test on geometry and the scanners' edge behavior use the comparison parameter "geometric truth". The measurements on the "braker plate" specimen have been done simultaneously with the noise parameter measurements. The intervals in range at the testing site were $\Delta_{DIST} = 20$ m. The data was converted as described above and evaluated with in-house software. The comparison parameter $n_{richtig}$ [%] is the percentage of geometrically correct points located within a $\pm 3\sigma_{DIST}$ confidence interval around the test body geometry. In the evaluation of the scanners' edge behavior especially the impact of the scan quality settings acting like smoothing filters and of the import filters will be regarded with respect to target distance. The point of view here is purely empirically as we do not use reference edges with known inter-distances.

In fig. 19 point clouds of the scanners are shown at 20 m and 100 m range with medium scan quality setting $f_{DIST} = 50\%$ and standard import filtering as examples.

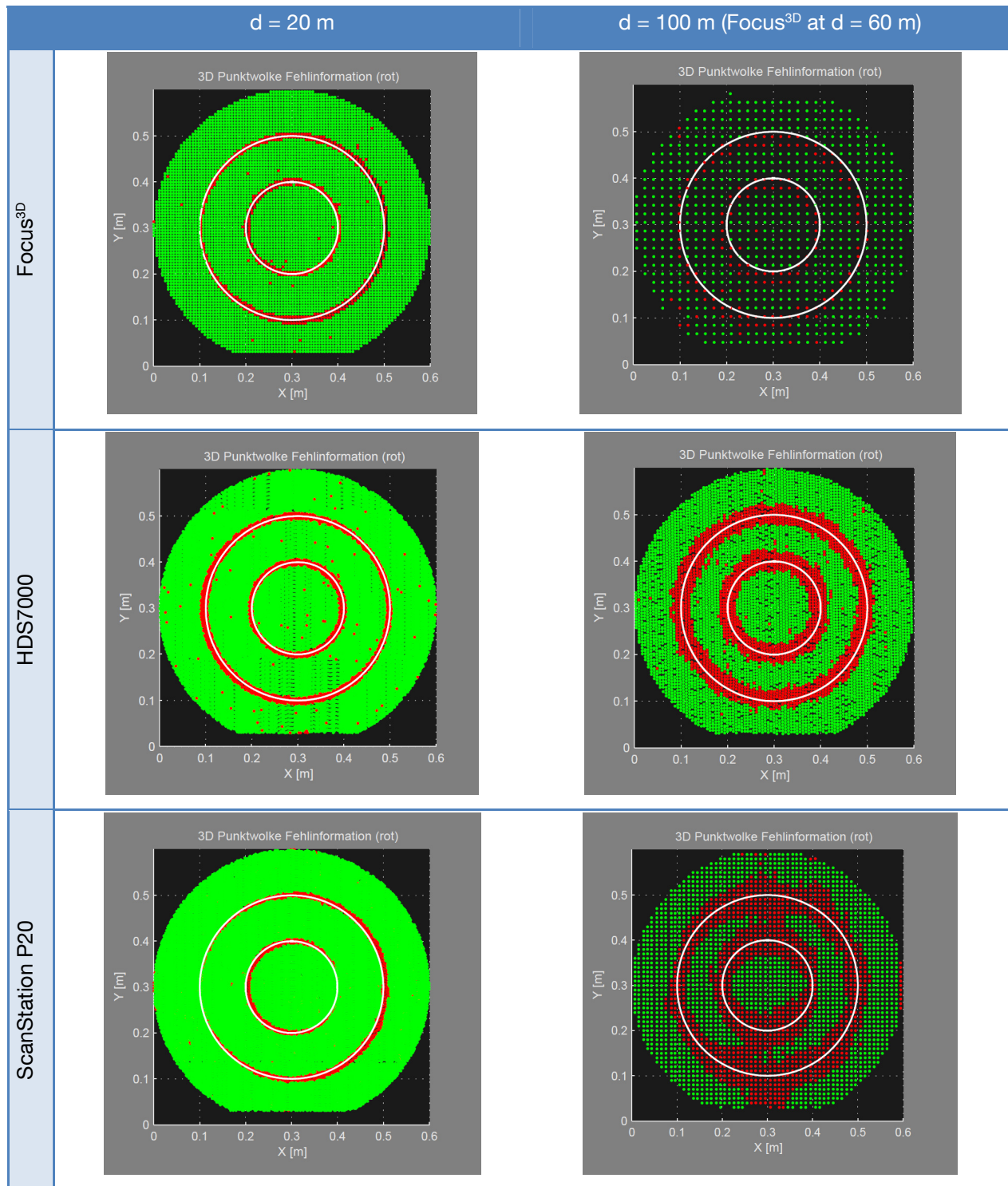


Figure 19: Edge behavior at the „breaker plate“ specimen

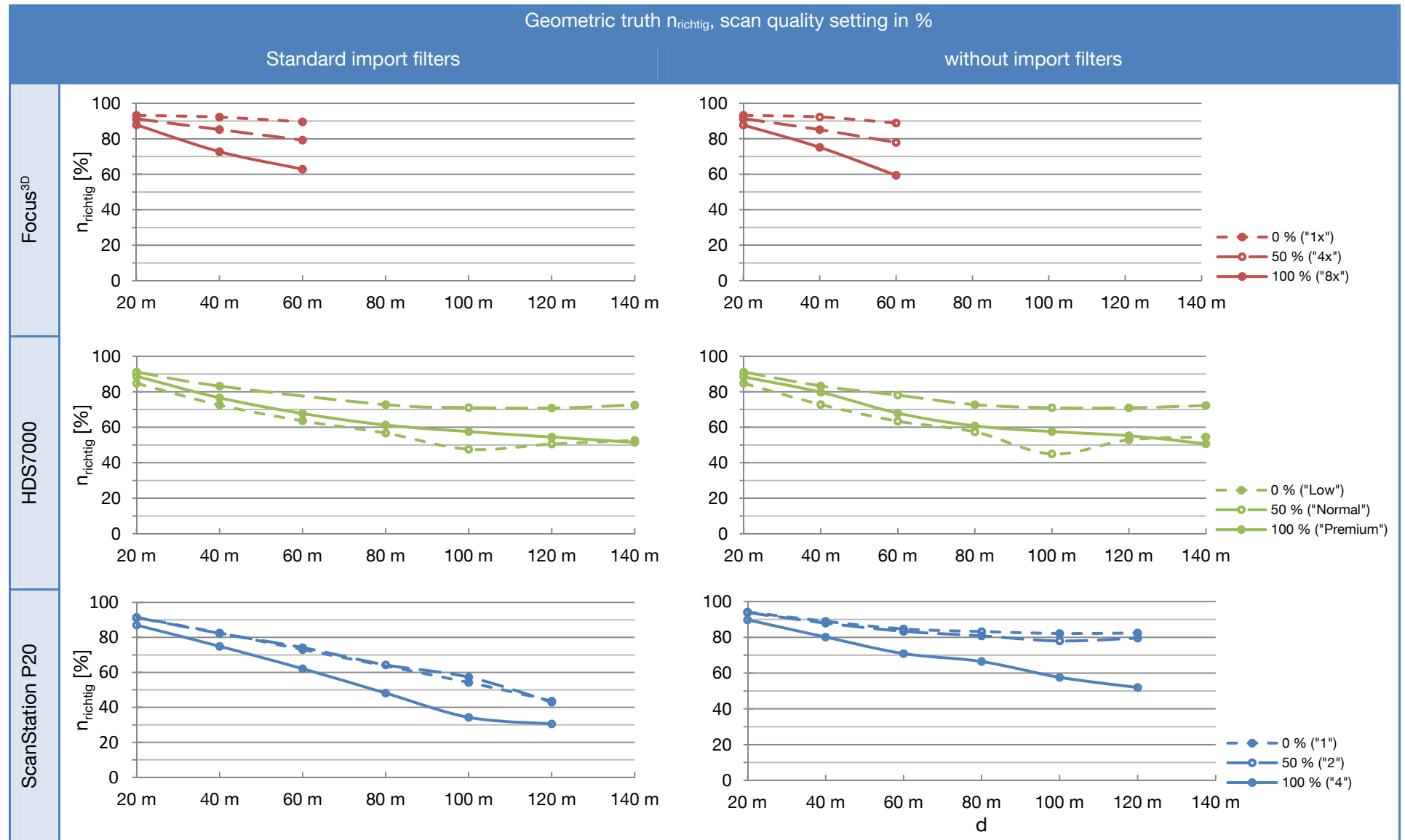


Figure 20: Geometric truth n_{richtig}

4.9 Working range

The defined comparison parameters “modelling range” d_{max} and “registration range” d_{ziel} have not been evaluated within the instrument comparison test. This is actually been done within a bachelor’s thesis („Investigation of target usage with laserscanners“) and will result in a guideline for the maximum allowable targeting distance with respect to scan quality settings. Results are expect until summer 2013.

Within the series at hand, the maximum possible measurement ranges for each specimen and scan quality setting can be given (table 6):

Table 6: Maximum working range on specimens:

TLS system	Import filter	f_{DIST} [%]	Working range [m] „breaker plate“	Working range [m] „board“
Focus ^{3D}	yes	0	60	70
		50		150
		100		70
	no	0		150
		50		150
		100		80
HDS7000	yes	0	140	150
		50		180
		100		170
	no	0		170
		50		180
		100		180
ScanStation P20	yes	0	120	120
		50		
		100		
	no	0		
		50		
		100		



4.10 Time of data acquisition

As mentioned earlier, comparable settings in scan resolution (approx. $r = 5 \text{ mm}/10 \text{ m}$) and a medium scan quality setting $f_{\text{DIST}} = 50 \%$ have been chosen. For the resolution, with each instrument we took the setting being closest to the value r . The measurement times t_{typisch} have been taken from the data sheets. Our tests have confirmed the provided information in all specifications.

Table 7: Typical time of data acquisition (HDS7000, Focus^{3D} and ScanStation P20)

TLS-System	r [mm/10 m]	f_{DIST} [%]	t_{typisch} [min:s]
Focus ^{3D}	6,136 („1/4“)	50 („4x“)	07:09
HDS7000	6,3 („High“)	50 („Normal quality“)	03:22
ScanStation P20	5 („5“)	50 („2“)	02:42

The comparison shows the HDS7000 and the ScanStation P20 with nearly equal speed, while the Focus^{3D} is slower at about factor 2.

4.11 Impact of potential obstructions at the specimens

During evaluation we considered it possible, that some objects which had to be attached to the specimens (aluminium parts, targeting markers) could affect the measurements. To overcome that, only areas in the center part of the specimens have been used and boundary parts with possible interfering reflections were eliminated (see fig. 21). At greater distances, areas of influences originating from obstructive objects can be seen in the point clouds, but they mostly don't reach the testing areas. Figure 21 shows the point clouds at the "board" specimen at 20 m and 100 m distance.

We also did additional laboratory tests using the HDS7000, where we covered obstructions with white paper. The resulting difference of the noise σ_{DIST} was negligible.

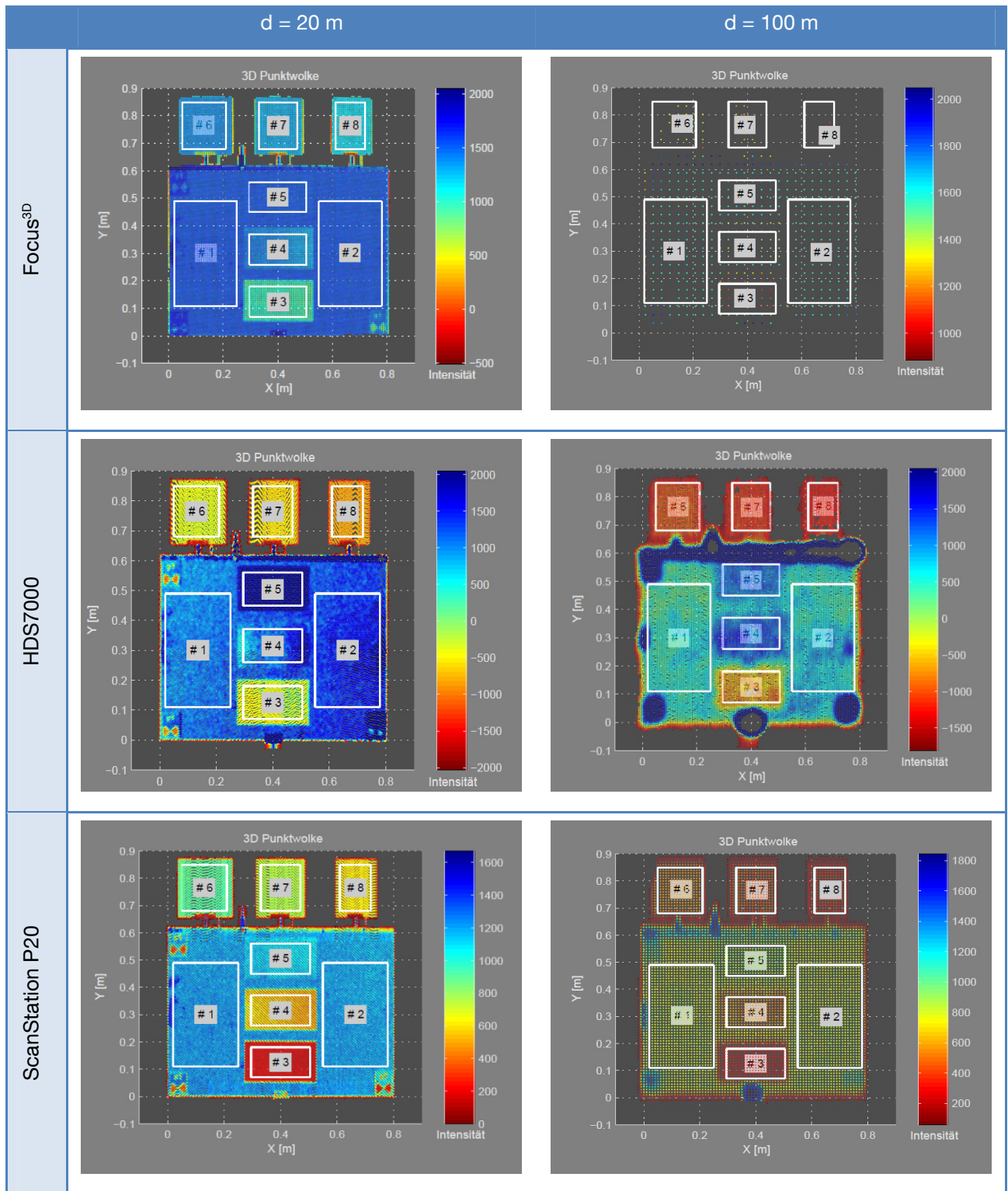


Figure 21: Point clouds on the „board“ specimen at $f_{DIST} = 50\%$ and with standard import filter settings.

4.12 Summary

The results show the different impact of the instruments' data filtering (scan quality settings) at acquisition time and of additional software import filters on the point cloud quality of three selected scanner models. The comparison concept shown here is meant as an additional con-



tribution towards standardized TLS specifications (e.g. a normalized comparison parameter for the range-dependent ranger noise is needed). For this, existing suggestions for TLS testing have been recapitulated at first, and new testing methods for special questions (especially filtering and edges) have been introduced.

5 Outlook

To promote an ISO standard (with strong European contribution), in a current PhD thesis „Calibration, registration and uniform quality measures in TLS“ at the Chair of Geodesy at the Technische Universität München existing international approaches are evaluated and improved.

Literature

BÖHLER, W. (2005): Vergleichende Untersuchungen zur Genauigkeit und Auflösung von Laserscannern. In: Deutscher Verein für Vermessungswesen (Eds.): Terrestrisches Laserscanning (TLS) – Ein geodätisches Messverfahren mit Zukunft, DVW-Schriftenreihe volume 48/2005. Augsburg: Wißner, 17–28.

CREMER (2013): Homepage Cremer Programmentwicklung GmbH, <http://www.cpentw.de>, accessed 02/01/2013.

FARO (2011): Faro Laser Scanner Focus^{3D} - manual, version october 2011.

FARO (2013): Homepage Faro - 3D-Messsysteme, europe.faro.com, accessed 01/28/2013.

FELDMANN, E.; PETERSEN, M.; STAIGER, R. (2011): Erste Erfahrungen mit Feldprüfverfahren für terrestrische Laserscanner. In: Deutscher Verein für Vermessungswesen (Hrsg.): Terrestrisches Laserscanning – TLS 2011 mit TLS-Challenge. DVW-Schriftenreihe volume 66/2011. Augsburg: Wißner, 77-96.

GORDON, B. (2008): Zur Bestimmung von Messunsicherheiten terrestrischer Laserscanner. Technische Universität Darmstadt, Fachbereich Bauingenieurwesen und Geodäsie, Dissertation. In: Online Publikationen der Technischen Universität Darmstadt, <http://tuprints.ulb.tu-darmstadt.de/1206/>, accessed 01.02.2013.

GOTTWALD, R. (2008): Field Procedures for Testing Terrestrial Laser Scanners (TLS), A Contribution to a Future ISO Standard. In: Proceedings of FIG Working Week 2008 Stockholm. http://www.fig.net/pub/fig2008/papers/ts02d/ts02d_02_gottwald_2740.pdf, accessed 01/23/2013.

GOTTWALD, R.; HEISTER, H.; STAIGER, R. (2008): Zur Prüfung und Kalibrierung von terrestrischen Laserscannern – eine Standortbestimmung. In: Deutscher Verein für Vermessungswesen (Hrsg.): Terrestrisches Laserscanning (TLS 2008). DVW-Schriftenreihe volume 54/2008. Augsburg: Wißner, 91-110.

HEISTER, H. (2006): Zur standardisierten Überprüfung von terrestrischen Laserscannern (TLS). In: Deutscher Verein für Vermessungswesen (Hrsg.): Terrestrisches Laser-Scanning (TLS 2006), DVW-Schriftenreihe volume 51/2006. Augsburg: Wißner, 35–44.

HESSE, Ch. (2008): Hochauflösende kinematische Objekterfassung mit terrestrischen Laserscannern. Gottfried Wilhelm Leibniz Universität Hannover, Fakultät für Bauingenieurwesen und Geodäsie, Dissertation. In: Wissenschaftliche Arbeiten der Fachrichtung Geodäsie und Geoinformatik der Leibniz Universität Hannover, volume 268.

HUXHAGEN, U.; SIEGRIST, B.; KERN, F. (2009): Vorschlag für eine TLS-Prüfrichtlinie. In: Luhmann, T. (Hrsg.) und Müller, Ch. (Eds.): Photogrammetrie, Laserscanning, Optische 3D-Messtechnik. Heidelberg: Wichmann, 3-12.



KERN, F. (2008): Prüfen und Kalibrieren von terrestrischen Laserscannern. In: Luhmann, Th. (Hrsg.); Müller, Ch. (Eds.): *Photogrammetrie, Laserscanning, Optische 3D-Messtechnik*. Heidelberg: Wichmann, 306-316.

KERN, F. (2010): Prüfrichtlinie zur Abnahme und Überwachung von terrestrischen Laserscanner-Systemen (Entwurf V.1.0.1), *Offenes Forum Terrestrisches Laserscanning*, http://www.laserscanning.org/documents/TLSRichtlinie_07.pdf, accessed 01/23/2013.

KERN, F.; HUXHAGEN, U. (2008): Ansätze zur systematischen Prüfung und Kalibrierung von terrestrischen Laserscannern. In: Deutscher Verein für Vermessungswesen (Eds.): *Terrestrisches Laserscanning (TLS 2008)*, DVW-Schriftenreihe volume 54/2008. Augsburg: Wißner, 111-124.

KERN, F. (2011): Praktische Erfahrung bei der TLS-Prüfung. 4. *Hamburger Anwendungsforum Terrestrisches Laserscanning am 23.06.2011, HafenCity Universität Hamburg, Presentation*. <http://www.i3mainz.fh-mainz.de>, accessed 01/23/2013.

LEICA (2011): HDS7000 – Gebrauchsanweisung, Version 1.0. http://www.leica-geosystems.com/downloads123/hds/general/HDS7000/manuals/HDS7000_UserManual_de.pdf, accessed 01/29/2013.

LEICA (2012): Leica ScanStation P20 – Industry’s Best Performing Ultra-High Speed Scanner, Data sheet. hds.leica-geosystems.com/downloads123/hds/hds/ScanStation_P20/brochures-datasheet/Leica_ScanStation_P20_DAT_en.pdf, accessed 01/29/2013.

LEICA (2013): Homepage Leica Geosystems – HDS. hds.leica-geosystems.com, accessed 01/28/2013.

LINDSTAEDT, M., KERSTEN, TH., MECHELKE, K., GRAEGER, T. (2012): Prüfverfahren für terrestrische Laserscanner – Gemeinsame geometrische Genauigkeitsuntersuchungen verschiedener Laserscanner an der HCU Hamburg. In: Th. Luhmann (Hrsg.), Ch. Müller (Eds.): *Photogrammetrie, Laserscanning, Optische 3D-Messtechnik - Beiträge der Oldenburger 3D-Tage 2012*. Berlin: Wichmann, 264-275.

NEITZEL, F. (2006): Gemeinsame Bestimmung von Ziel-, Kippachsenfehler und Exzentrizität der Zielachse am Beispiel des Laserscanners Zoller + Fröhlich Imager 5003. In: Luhmann, Th. (Hrsg.); Müller, Ch. (Eds.): *Photogrammetrie, Laserscanning, Optische 3D-Messtechnik*. Berlin: Wichmann, 174-183.

NEITZEL ET AL. (2013): Verfahren zur standardisierten Überprüfung von terrestrischen Laserscannern. In: Deutscher Verein für Vermessungswesen (Ed.): *DVW-Merkblatt (in progress)*.

REIDL, F. (2012): Konzept und Durchführung einer Systemkalibrierung von terrestrischen Laserscannern. Technische Universität München, Lehrstuhl für Geodäsie. Master thesis, unpublished.

SHAN, J.; TOTH, C. K. (2009): *Topographic Laser Ranging and Scanning – Principles and Processing*. Boca Raton: CRC Press.



STAIGER, R. (2005): Terrestrisches Laserscanning – Eine neue Universalmethode? In: Deutscher Verein für Vermessungswesen (Hrsg.): Terrestrisches Laserscanning (TLS 2008), DVW-Schriftenreihe volume 54/2008. Augsburg: Wißner, 3-16.

TÜXEN, H. (2008): Ideas for field procedure to test Terrestrial Laser Scanners (TLS). Offenes Forum Terrestrisches Laserscanning, Beitrag zur 1. Sitzung vom 02.09.2008.
http://www.laserscanning.org/Sitzung1/PDF/2008-09-02Tuexen-Proposal-for-field-procedure-to-test-TLS_5.pdf, accessed 01/23/2013.

VDI/VDE 2634 (2012): Optische 3-D-Messsysteme, Bildgebende Systeme mit flächenhafter Abtastung – Blatt 2, VDI/VDE-Richtlinie 2634, Version august 2012, Beuth, Berlin.

WEHMANN, W. (2007): Einrichtung eines Prüffeldes zur Genauigkeitsbestimmung von Laserscannern und Untersuchung des Scanners LMS-Z360i der Firma Riegler in diesem Testfeld. In: zfv (132/3), 175-180.

WEHMANN, W. (2008): Untersuchungen zu geeigneten Feldverfahren zur Überprüfung Terrestrischer Laserscanner. Offenes Forum Terrestrisches Laserscanning, Beitrag zur 1. Sitzung vom 02.09.2008.
<http://www.laserscanning.org/Sitzung1/PDF/2008-09-02Wehmann-Feldverfahren-zur-TLS-Pruefung.pdf> accessed 01/23/2013.

WUNDERLICH, TH. (2012): Objektivierung von Spezifikationen Terrestrischer Laserscanner, Ein Beitrag des Geodätischen Prüflabors der Technischen Universität München. INTERGEO – Kongress und Fachmesse für Geodäsie, Geoinformation und Landmanagement, Presentation, Hannover, 08.10.2012